Inorg. Chem. **2002**, *41*, 3560–3569

Metal Cyanide Ions $M_x(CN)_y]^{+,-}$ in the Gas Phase: M = Fe, Co, Ni, Zn, Cd, Hg, Fe + Ag, Co + Ag

Ian G. Dance,* Philip A. W. Dean,*[,1] Keith J. Fisher, and Hugh H. Harris

School of Chemistry, University of New South Wales, Sydney NSW 2052, Australia

Received November 30, 2001

The generation of metal cyanide ions in the gas phase by laser ablation of $M(CN)_2$ (M = Co, Ni, Zn, Cd, Hg), $Fe^{III}[Fe^{III}(CN)_6]\cdot xH_2O$, $Ag_3[M(CN)_6]$ (M = Fe, Co), and $Ag_2[Fe(CN)_5(NO)]$ has been investigated using Fourier transform ion cyclotron resonance mass spectrometry. Irradiation of $Zn(CN)_2$ and $Cd(CN)_2$ produced extensive series of anions, $[Zn_n(CN)_{2n+1}]^-$ ($1 \le n \le 27$) and $[Cd_n(CN)_{2n+1}]^-$ (n = 1, 2, 8–27, and possibly 29, 30). Cations $Hg(CN)^+$ and $[Hg_2(CN)_x]^+$ (x = 1–3), and anions $[Hg(CN)_x]^-$ (x = 2, 3), are produced from $Hg(CN)_2$. Irradiation of Fe^{III}-$[Fe^{III}(CN)_6]\cdot xH_2O$ gives the anions $[Fe(CN)_2]^-$, $[Fe(CN)_3]^-$, $[Fe_2(CN)_3]^-$, $[Fe_2(CN)_4]^-$, and $[Fe_2(CN)_5]^-$. When Ag_3-$[Fe(CN)_6]$ is ablated, $[AgFe(CN)_4]^-$ and $[Ag_2Fe(CN)_5]^-$ are observed together with homoleptic anions of Fe and Ag. The additional heterometallic complexes $[AgFe_2(CN)_6]^-$, $[AgFe_3(CN)_8]^-$, $[Ag_2Fe_2(CN)_7]^-$, and $[Ag_3Fe(CN)_6]^-$ are observed on ablation of $Ag_2[Fe(CN)_5(NO)]$. Homoleptic anions $[Co_n(CN)_{n+1}]^-$ (n = 1–3), $[Co_n(CN)_{n+2}]^-$ (n = 1–3), $[Co_2(CN)_4]^-$, and $[Co_3(CN)_5]^-$ are formed when anhydrous $Co(CN)_2$ is the target. Ablation of $Ag_3[Co(CN)_6]$ yields cations $[Ag_n(CN)_{n-1}]^+$ (n = 1–4) and $[Ag_nCo(CN)_n]^+$ (n = 1, 2) and anions $[Ag_n(CN)_{n+1}]^-$ (n = 1–3), $[Co_n(CN)_{n-1}]^-$ (n = 1, 2), $[Ag_nCo(CN)_{n+2}]^-$ (n = 1, 2), and $[Ag_nCo(CN)_{n+3}]^-$ (n = 0–2). The Ni(I) species $[Ni_n(CN)_{n-1}]^+$ (n = 1–4) and $[Ni_n(CN)_{n+1}]^-$ (n = 1–3) are produced when anhydrous $Ni(CN)_2$ is irradiated. In all cases, CN^- and polyatomic carbon nitride ions $C_xN_y^-$ are formed concurrently. On the basis of density functional calculations, probable structures are proposed for most of the newly observed species. General structural features are low coordination numbers, regular trigonal coordination stereochemistry for d^{10} metals but distorted trigonal stereochemistry for transition metals, the occurrence of M–CN–M and M(–CN–)$_2$M bridges, addition of AgCN to terminal CN ligands, and the occurrence of high spin ground states for linear $[M_n(CN)_{n+1}]^-$ complexes of Co and Ni.

Introduction

In a previous paper,[2] we reported that laser ablation (LA) of MCN (M = Cu, Ag) yielded the gaseous ions $[M_n(CN)_{n-1}]^+$ and $[M_n(CN)_{n+1}]^-$, characterized by Fourier transform ion cyclotron resonance mass spectrometry (FTICR MS). Geometry optimizations using density functional theory showed that the most stable structures for the Cu(I) ions are linear alternations of Cu and CN, even at the highest values of n observed (n = 6 for $[Cu_n(CN)_{n-1}]^+$, n = 5 for $[Cu_n(CN)_{n+1}]^-$). The occurrence of these very long straight molecules, one atom thick, is consistent with the propensity of CN^- to participate in linear M−CN−M bridging, as opposed to M−C(N)−M bridging or other bridging modes. Laser ablation of zinc and cadmium cyanides $M(CN)_2$ yielded extended series of ions $[M_n(CN)_{2n+1}]^-$ (up to n = 27), for which density functional and force-field calculations indicated the occurrence of helical structures formed by almost linear M−(μ-CN)−M linkages of three-coordinate (μ-CN)$_2$-MCN units.[3]

Following the results for gas-phase cyano complexes of Cu(I), Ag(I), Zn(II), and Cd(II), and the tendency of CN^- to form linear bridges, we expected that further binary metal−cyanide clusters and structures could be generated in the gas phase. Intriguing polycyanometalate molecular clusters such as $[Mn\{Mn(MeOH)_3\}_8(\mu\text{-}CN)_{30}\{Mo(CN)_3\}_6]$,[4] $[(Me_3tacn)_8Cr_8Ni_6(CN)_{24}]^{12+}$,[5] and $Cr_8Ni_5(CN)_{24}$ and $Cr_{10}Ni_9(CN)_{42}$ [6] clusters in crystals have been reported recently.

* To whom correspondence should be addressed. E-mail: i.dance@unsw.edu.au (I.G.D.); pawdean@julian.uwo.ca (P.A.W.D.).

(1) On leave from The University of Western Ontario, London, Ontario N6A 5B7, Canada.

(2) Dance, I. G.; Dean, P. A. W.; Fisher, K. J. *Inorg. Chem.* **1994**, *33*, 6261−6269.

(3) Dance, I. G.; Dean, P. A. W.; Fisher, K. J. *Angew. Chem., Int. Ed. Engl.* **1995**, *34*, 314−316.

(4) Larionova, J.; Gross, M.; Pilkington, M. J.; Andres, H.; Stoeckli-Evans, H.; Gudel, H. U.; Decurtins, S. *Angew. Chem., Int. Ed.* **2000**, *39*, 1605−1609.

10.1021/ic011227d CCC: $22.00
Published on Web 06/07/2002

Accordingly, we extended our ablation studies to include the cyanides of mercury and of transition metals with different oxidation states and coordination chemistry. We present here a fuller account of our LA FTICR MS studies of $M(CN)_2$ (M = Zn or Cd) and new LA FTICR MS data for $M(CN)_2$ (M = Hg, Co, Ni), $Fe^{III}[Fe^{III}(CN)_6]\cdot xH_2O$.[7a] $Fe(CN)_2$ is not well characterized.[7a] We have also investigated mixed-metal cyanides in the gas phase, using solid $Ag_3[M(CN)_6]$ (M = Fe, Co), and $Ag_2[Fe(CN)_5(NO)]$ as precursors.

Finally, we report calculations by density functional theory of the possible structures of many of the ions that we observe, and we compare what we have observed in the gas phase with the known structural chemistry of cyanide complexes of the various central elements in condensed phases. Many crystalline cyanocomplexes have interesting structures and magnetic properties.[4−6,8]

Experimental Section

CAUTION! Metal cyanides and most cyanometalates are toxic and should be handled and disposed of accordingly.

Materials. Sodium cyanide (Mallinckrodt), $ZnSO_4\cdot 7H_2O$ (Ajax Chemicals), and $Cd(NO_3)_2\cdot 4H_2O$ (BDH) were analytical reagents and were used as received, as were reagent-grade $AgNO_3$ (Ajax Chemicals), $Ni(NO_3)_2\cdot 6H_2O$, $CoSO_4\cdot 7H_2O$, and $K_3Fe(CN)_6$ (all from M and B), $Hg(CN)_2$ (BDH), and $Na_2[Fe(CN)_5(NO)]\cdot 2H_2O$. The literature method was used to prepare $K_3[Co(CN)_6]$.[9]

Syntheses. Zinc cyanide was precipitated by stirring an aqueous solution containing the stoichiometric quantity of NaCN into an aqueous solution of $ZnSO_4\cdot 7H_2O$.[7b] Cadmium cyanide and hydrated $Ni(CN)_2$ were prepared similarly from NaCN and the appropriate metal nitrate.[7b,c] Hydrated $Co(CN)_2$ was synthesized similarly, but by using solutions that had been deoxygenated using a flow of $N_2(g)$.[7d]

Colorless $Zn(CN)_2$ and $Cd(CN)_2$ were separated by filtration, washed three times with water and three times with acetone, and then dried in vacuo. The very fine precipitate of hydrated $Ni(CN)_2$ was separated by centrifugation, washed three times with water and twice with EtOH, recentrifuging after each wash, and then dried in vacuo. Yellow-brown anhydrous $Ni(CN)_2$ was obtained by heating the hydrated material at 150 °C overnight.[7c] Pink-beige hydrated $Co(CN)_2$ was also separated by centrifugation. It was washed three times with water, and the final slurry was converted to deep blue anhydrous $Co(CN)_2$ by slowly heating it to 250 °C under a flow of $N_2(g)$.[7d] Anhydrous $Co(CN)_2$ is very easily rehydrated and was handled thereafter in a glovebag under $N_2(g)$.

$Fe^{III}[Fe^{III}(CN)_6]\cdot xH_2O$ was produced by heating an aqueous solution of $FeCl_3$ and $K_3Fe(CN)_6$ (3:1) at 90 °C in the dark for several hours.[7e] The very fine deep green product was separated by centrifugation, washed three times with water and twice with EtOH, and then dried in vacuo.

The silver salts $Ag_3[M(CN)_6]$ (M = Fe, Co) and $Ag_2[Fe(CN)_5(NO)]$ precipitated on mixing aqueous solutions of $Ag(NO_3)$ and the appropriate $K_3[M(CN)_6]$ or $Na_2[Fe(CN)_5(NO)]\cdot 2H_2O$ in a foil-covered beaker. They were washed with water and then EtOH and dried under vacuum.

LA FTICRMS. Sample preparation and the apparatus and techniques used for the laser ablation and mass spectrometry have been described previously in papers from these laboratories.[2,10] The LA FTICR mass spectra of all of the cyanides were surveyed at both 1064 and 532 nm using a Q-switched YAG laser. Power densities available were in the range $1.3-85 \times 10^3$ MW cm^{-2} at 1064 nm and 2.4−77 MW cm^{-2} at 532 nm (assuming a typical spot size of 0.2 mm diameter). Typically, nominal starting power levels in an experiment were 1.7×10^3 MW cm^{-2} at 1064 nm and 11 MW cm^{-2} at 532 nm, and the spectra were optimized in terms of the number of species observed and the signal/noise (S/N) by adjusting the laser power. Approximate actual power levels were calculated using the average energy of the laser pulse, measured with a joule-meter, and the actual size of the irradiated spot at the end of the experiment, measured with a microscope. The same ions were observed using both 1064 and 532 nm irradiation, except as noted in Table 1.

An ion was considered observed if it occurred with $S/N \geq 2$ over several repetitions of the spectral measurement. For experiments involving collision-induced dissociation (CID), the collision gas, Ar, (CCl_4 was also used for the $C_xN_y^-$ anions) was present at a pressure of 1×10^{-7} mbar. Ions for CID were selected and all unwanted ions removed from the cell. The selected ions were accelerated with an rf excitation pulse and allowed to have ∼1 collision (0.02−0.05 s) before observation of the product ions. The short collision time was used to avoid secondary collisions and also to reduce the possibility of ion rearrangement. Collision energies given in the Results and Discussion sections are center-of-mass collision energies giving ca. 50% dissociation.

In general, the spectra from the initial laser shots were not representative of those from the later shots, a common situation during laser ablation studies.[11] The laser hits one spot, and the resulting surface modification presumably leads to the observed spectral changes. The spectra that we show are representative of those obtained from approximately the 5th laser shot through to the 20th laser shot.

Density Functional Calculations. Calculations were with the program DMol3,[12] using the double numeric basis sets[12a] including polarization functions (basis set type DND). The calculations were all-electron and were unrestricted for all species not having a well-defined closed shell. Scalar relativistic corrections to the core orbitals were included for the all-electron calculations for the mercury species. Becke 88 exchange and Lee−Yang−Parr correlation functionals[13] were used throughout. The calculational strategy involved geometry optimization for numerous postulated

(5) Berseth, P. A.; Sokol, J. J.; Shores, M. P.; Heinrich, J. L.; Long, J. R. *J. Am. Chem. Soc.* **2000**, *122*, 9655−9662.
(6) Sokol, J. L.; Shores, M. P.; Long, J. R. *Angew. Chem., Int. Ed.* **2001**, *40*, 236−239.
(7) Sharpe, A. G. *The Chemistry of the Cyano Complexes of the Transition Elements*; Academic Press: London, 1976. (a) Page 103 ff and references therein. (b) Page 287 ff. (c) Page 231 ff and references therein. (d) Page 166 ff and references therein. (e) Page 123 ff and references therein. (f) Page 103 ff and references therein. (g) Page 101 ff and references therein. (h) Page 162 ff and references therein. (i) Page 228 ff and references therein.
(8) Dunbar, K. R.; Heintz, R. A. *Prog. Inorg. Chem.* **1997**, *45*, 283−391. Miller, J. S.; Manson, J. L. *Acc. Chem. Res.* **2001**, *34*, 563−570. Cernak, J.; Orenda, M.; Potocnak, I.; Chomic, J.; Orendacova, A.; Skorsepa, J.; Feher, A. *Coord. Chem. Rev.* **2002**, *224*, 51−66.
(9) Bigelow, J. H. *Inorg. Synth.* **1946**, *2*, 225−227.
(10) El Nakat, J. H.; Dance, I. G.; Fisher, K. J.; Rice, D.; Willett, G. D. *J. Am. Chem. Soc.* **1991**, *113*, 5141−5148. El Nakat, J. H.; Fisher, K. J.; Dance, I. G.; Willett, G. D. *Inorg. Chem.* **1993**, *32*, 1931−1940. Dance, I. G.; Fisher, K. J.; Willett, G. D. *J. Chem. Soc., Dalton Trans.* **1997**, 2557−2561.
(11) Campbell, E. E. B.; Hasselberger, B.; Ulmer, G.; Busmann, H. G.; Hertel, I. V. *J. Chem. Phys.* **1990**, *93*, 6900−7; Pozniak, B.; Dunbar, R. C. *Int. J. Mass Spectrom.* **1994**, *133*, 97−110.
(12) (a) Delley, B. *J. Chem. Phys.* **1990**, *92*, 508−517. (b) Delley, B. In *Modern density functional theory: a tool for chemistry*; Seminario, J. M., Politzer, P., Eds.; Elsevier: Amsterdam, 1995; Vol. 2; pp 221−254. (c) MSI, http://www.msi.com.

Table 1. Metal-Containing Ions Observed after Laser Ablation of $M(CN)_2$ (M = Co, Ni, Zn, Cd, Hg), "$Fe[Fe(CN)_6]\cdot xH_2O$", $Ag_3[M(CN)_6]$ (M = Fe,Co), and $Ag_2[Fe(CN)_5(NO)]$[a,b]

metal(s)	positive ions	negative ions
Zn	Zn^+, Zn_2^+,[c] $[Zn(CN)]^+$ [c]	$[Zn_n(CN)_{2n+1}]^-$ ($n = 1-27$)[d,e]
Cd	Cd^+, Cd_2^+, $[Cd(CN)]^+$	$[Cd_n(CN)_{2n+1}]^-$ ($n = 1, 2, 8-27, 29, 30$)[f]
Hg	Hg^+, Hg_2^+, $[Hg(CN)]^+$, $[Hg_2(CN)]^+$,[g] $[Hg_2(CN)_2]^+$,[g] $[Hg_2(CN)_3]^+$ [g]	Hg^-, $[Hg(CN)_2]^-$, $[Hg(CN)_3]^-$
Fe[h]	Fe^+	$[Fe(CN)_2]^-$, $[Fe(CN)_3]^-$, $[Fe_2(CN)_3]^-$,[g] $[Fe_2(CN)_4]^-$,[g] $[Fe_2(CN)_5]^-$ [g]
Co	Co^+	$[Co(CN)_2]^-$, $[Co(CN)_3]^-$, $[Co_2(CN)_3]^-$, $[Co_2(CN)_4]^-$, $[Co_3(CN)_4]^-$, $[Co_3(CN)_5]^-$
Ni	Ni^+, $[Ni_2(CN)]^+$, $[Ni_3(CN)_2]^+$, $[Ni_4(CN)_3]^+$ [g]	$[Ni(CN)_2]^-$, $[Ni_2(CN)_3]^-$, $[Ni_3(CN)_4]^-$
Fe, Ag[i]	K^+,[g] Fe^+,[g] Ag^+, $[Ag_2(CN)]^+$,[c] $[Ag_3(CN)_2]^+$,[c] $[Ag_4(CN)_3]^+$ [c]	$[Ag(CN)_2]^-$, $[Ag_2(CN)_3]^-$, $[Ag_3(CN)_4]^-$, $[Fe(CN)_3]^-$, $[AgFe(CN)_4]^-$, $[Ag_2Fe(CN)_5]^-$
Fe, Ag[j]	Na^+, Fe^+, Ag^+	$[Ag(CN)_2]^-$, $[Ag_2(CN)_3]^-$, $[Ag_3(CN)_4]^-$, $[Fe(CN)_3]^-$,[c] $[Fe_2(CN)_3]^-$,[c] $[Fe_2(CN)_5]^-$,[c] $[Fe_3(CN)_7]^-$,[c] $[AgFe_2(CN)_6]^-$,[c] $[Ag_2Fe_2(CN)_7]^-$,[c] $[AgFe(CN)_4]^-$,[c] $[Ag_2Fe(CN)_5]^-$,[c] $[Ag_3Fe(CN)_6]^-$,[c] $[AgFe_3(CN)_8]^-$ [c]
Co, Ag[k]	K^+,[g] Co^+,[g] Ag^+, Ag_2^+, $[Ag_2(CN)]^+$,[c] $[Ag_3(CN)_2]^+$,[c] $[Ag_4(CN)_3]^+$,[c] $[AgCo(CN)]^+$,[c] $[Ag_2Co(CN)_2]^+$ [c]	Ag^-, $[Co(CN)_2]^-$, $[Co_2(CN)_3]^-$, $[Ag(CN)_2]^-$, $[Ag_2(CN)_3]^-$, $[Ag_3(CN)_4]^-$, $[AgCo(CN)_3]^-$, $[Ag_2Co(CN)_4]^-$,[c] $[AgCo(CN)_4]^-$,[c] $[Ag_2Co(CN)_5]^-$ [c]

[a] See text. Varying amounts of CN^- and polyatomic $C_xN_y^-$ are produced also. [b] Species listed are those observed using both 1064 and 532 nm irradiation, except as noted. [c] Not observed with 532 nm irradiation. [d] See Figure 1. [e] Species with $n = 2-27$ not observed at 532 nm. [f] Only the anions with $n = 1, 2$ observed with 532 nm irradiation. [g] Observed with 532 nm irradiation only. [h] From $Fe^{III}[Fe^{III}(CN)_6]\cdot xH_2O$. [i] From $Ag_3[Fe(CN)_6]$. HCN-containing cations are detected also (see text). [j] From $Ag_2[Fe(CN)_5(NO)]$. [k] From $Ag_3[Co(CN)_6]$.

structures, without specification of the electronic state, so that the lowest energy electronic configuration is obtained. In addition, smearing techniques allowing partial occupancy of orbitals in the vicinity of the Fermi level were incorporated during optimization.[12a,b] This permits the energy minimization to access alternative close-lying electronic states and to find the local minimum in geometry-electronic space (the charge smearing was reduced to zero for the final optimization of each species). Second derivative (frequency) calculations were not generally made to confirm that stationary points were true minima, but experience with the quality of the gradients during optimizations supports the assumption of true minima in most cases. Some species evidently possessed complex geometry-electronic surfaces, and these are identified in the presentation of results.

Results and Interpretation

General. The signals observed in the mass spectra of laser-ablated $M(CN)_2$ were assigned using a combination of mass and, for M = Ni, Zn, Cd, or Hg, the isotopomer patterns. Co is monoisotopic, and species produced from $Co(CN)_2$ were confirmed by measurement of exact masses. A summary of all metal-containing species detected is given in Table 1.

The ablation of most of the compounds studied here leads to varying amounts of polyatomic anions of the type $C_xN_y^-$, in addition to CN^- and M-containing species, for example,

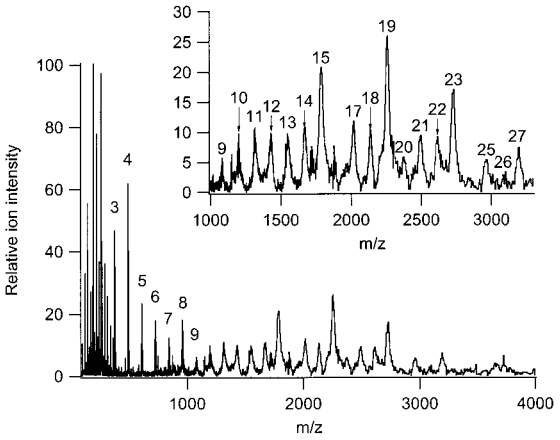

Figure 1. Negative ion mass spectrum obtained by the laser ablation of $Zn(CN)_2$ at 1064 nm with power density $\approx 1.8 \times 10^4$ MW cm^{-2}, showing the formation of $[Zn_n(CN)_{2n+1}]^-$ ($n = 1-27$) and (at $m/z < 200$) various $C_xN_y^-$. Inset is a 3.33× vertical expansion.

Figure 1. Evidently, some fragmentation of CN^- is occurring. These results contrast with the ablation of MCN (M = Cu, Ag) where such decomposition is not significant.[2] Several of the $C_xN_y^-$ obtained by ablation of $M(CN)_2$, namely C_xN^-, $x = 3, 7, 10$; $C_xN_2^-$, $x = 4, 6, 8, 10, 14, 16$; $C_xN_4^-$, $x = 6, 8, 10, 12, 14$; and $C_5N_5^-$, were studied in detail. However, partway through our investigation, reports were made[14,15] of $C_xN_y^-$ obtained by laser ablation of $K_3[Fe(CN)_6]$,[16,17] and thereafter, our detailed study of $C_xN_y^-$ was discontinued. The results for the anions that we observed are summarized in the Supporting Information. It should be mentioned that a different distribution of $C_xN_y^-$ anions is observed in the current work than after laser ablation of the $K_{3\text{ or }4}[M(CN)_6]$. Laser ablation of $Hg(CN)_2$ gives a particularly wide range of $C_xN_y^-$, which is consistent with the fact that *thermal* decomposition of $Hg(CN)_2$ yields cyanogen, $(CN)_2$, together with paracyanogen (which itself is appreciable degraded at 1200 °C).[18]

Precursors $Zn(CN)_2$ and $Cd(CN)_2$. Ablation of $M(CN)_2$ (M = Zn, Cd) using 1064 nm radiation gives a positive ion spectrum showing mainly M^+ but with minor amounts of M_2^+ and $[M(CN)]^+$. However, the negative ion spectra produced from these substrates with the IR laser are more remarkable. Figure 1 shows a spectrum for M = Zn, with the long series of ions $[Zn_n(CN)_{2n+1}]^-$ extending for 27 members from $[Zn(CN)_3]^-$ to $[Zn_{27}(CN)_{55}]^-$ ($n = 1-27$). The spectra of $C_xN_y^-$ (see previously) occur in the lower part of this mass range. High resolution spectra have been measured and satisfactorily simulated for the complexes with $n = 1-12$. The identities of the higher members of the series follow from the common mass separation, $\Delta(m/z) = 118$ units.

(13) Becke, A. D. *Phys. Rev. A* **1988**, *38*, 3098−3100. Lee, C.; Yang, W.; Parr, R. G. *Phys. Rev. B* **1988**, *37*, 785−789.

(14) Wang, C. R.; Huang, R. B.; Liu, Z. Y.; Zheng, L. S. *Chem. Phys. Lett.* **1995**, *237*, 463−467.

(15) Tang, Z.-C.; Huang, R.-B.; Shi, L.; Zheng, L.-S. *Int. J. Mass Spectrom.* **1998**, *173*, 71.

(16) In another study[17] of the laser ablation products of $K_3[Fe(CN)_6]$ by TOF MS, in which we presume lower power densities were used, $[K(KCN)_x]^+$ and $[(KCN)_x(CN)]^-$ were the ions detected.

(17) Zhang, X.-G.; Li, H.-Y.; Ma, C.-S.; Wang, X.-Y.; Bai, J.-L.; He, G.-Z.; Lou, N.-O. *Chem. Phys. Lett.* **1997**, *274*, 115.

(18) Brotherton, T. K.; Lynn, J. W. *Chem. Rev.* **1959**, *59*, 844 and references therein.

It is notable that the relative intensities of the ions in the series $[Zn_n(CN)_{2n+1}]^-$ are highest in the central region of the series, maximizing at $n = 15$, 19, 23 with odd numbers of metal atoms: this is unlike the commonly observed general reduction in intensity with increasing mass and signifies enhanced stability of ions $[Zn_n(CN)_{2n+1}]^-$ with $n \sim 19$. We note also that these ions all contain zinc in its normal +II oxidation state.

The only Zn-containing ions detected when $Zn(CN)_2$ was ablated using 532 nm radiation were Zn^+ and $[Zn(CN)_3]^-$.

Negative ion spectra obtained from $Cd(CN)_2$ using 1064 nm radiation also show the spectra of $C_xN_y^-$ at lower masses. Above $m/z \cong 1000$, an extended series of ions $[Cd_n(CN)_{2n+1}]^-$ is observed in which $n = 8-27$, and possibly 29, 30. The identity of the species with $n = 8$ was confirmed by a simulation of the isotopic pattern measured in the narrow-band spectrum. The identity of other members of the series follows from the common m/z separation of 164 units and by analogy with the better-characterized zinc analogues. When 532 nm radiation is used, the only cyano anions observed are $[Cd(CN)_3]^-$ and $[Cd_2(CN)_5]^-$, and Cd^+ is the sole cation.

There are several distinctive features of the spectra of the series $[Cd_n(CN)_{2n+1}]^-$. First, no evidence was found for members with $n < 8$ when 1064 nm radiation was used. This contrasts with the series $[Zn_n(CN)_{2n+1}]^-$ described previously. However, two of the missing members of the Cd series, those with $n = 1$, 2, are the only cyano complexes observed in the negative ion mass spectrum when ablation is carried out with 532 nm radiation. Second, there are regions of the spectrum where alternation of signal intensity occurs. In the region $n = 14-20$, the most prominent species with $n = 15$, 17, 19 again have an odd number of metal atoms, as is also found for their Zn congeners. In contrast, in the region $n = 8-14$, the most abundant species ($n = 8$, 10, 12, 14) have even numbers of metal atoms. Finally, we note that, as for the cyanozincates, the Cd complexes contain the metal in the formal +II oxidation state.

Precursor $Hg(CN)_2$. The positive ion mass spectrum obtained when $Hg(CN)_2$ is ablated at 1064 or 532 nm contains Hg^+ as a major ion and $[Hg(CN)]^+$ and Hg_2^+ as minor ions. When 532 nm radiation is used, the dimercury species $[Hg_2(CN)_x]^+$ ($x = 1-3$) are observed also (Figure 2). The cation $[Hg_2(CN)]^+$ invariably has low abundance and indeed does not occur in Figure 2, but the corresponding di- and tricyanides are the major species observed in some of the spectra. (The dependence of spectra on the extent of ablation has been mentioned.)

The complexes $[Hg(CN)_2]^-$ and $[Hg(CN)_3]^-$ are major anionic products of ablation using either 1064 or 532 nm radiation. There was no evidence for $[Hg(CN)]^-$. An additional species observed with both 1064 and 532 nm radiation was Hg^-.

Precursor $Fe^{III}[Fe^{III}(CN)_6]\cdot xH_2O$. Only Fe^+ was observed in the positive ion spectrum of this substance whether dried under vacuum alone or under vacuum and then at 200 °C. When relatively low laser power densities were used, evidence could be obtained for a limited series of Fe-containing anions. In our experiments, the best results were obtained using 532 nm radiation with irradiances 17−66 MW cm^{-2}. The complexes $[Fe(CN)_2]^-$ and $[Fe(CN)_3]^-$ were definitely established, with measurement of the signals from the ^{54}Fe-containing isotopomers. The species $[Fe_2(CN)_3]^-$, $[Fe_2(CN)_4]^-$, and $[Fe_2(CN)_5]^-$ were observed only as the most intense isotopomer. The ions $[Fe(CN)_2]^-$, $[Fe(CN)_3]^-$, and $[Fe(CN)_4]^-$ were detected in an earlier time-of-flight mass spectrometric (TOF MS) study of the products of laser ablation of $K_3[Fe(CN)_6]$ and $K_4[Fe(CN)_6]$.[15]

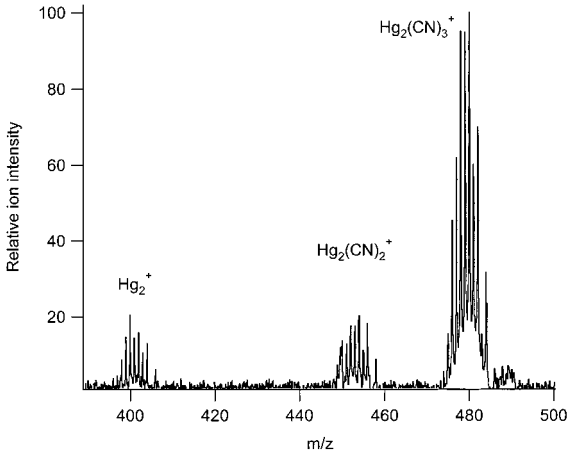

Figure 2. Positive ion mass spectrum obtained by the laser ablation of $Hg(CN)_2$ at 532 nm with power density ≈ 2.7 MW cm^{-2}, showing the formation of dimetallic cations.

Precursor $Ag_3[Fe(CN)_6]$. When ablation was carried out using 1064 nm irradiation, the cyano complexes that could be detected in the positive ion mass spectrum of this salt were the known cations $[Ag_n(CN)_{n-1}]^+$ ($n = 1-4$)[2] and several cations of formula $[Ag_n(CN)_{n-1}(NCH)_m]^+$, for example, $[Ag_2(CN)(NCH)]^+$, $[Ag_3(CN)_2(NCH)_m]^+$ ($m = 1$, 2): the resolution was more than sufficient to detect a difference of 1 mass unit. These HCN complexes indicate the presence of a proton source even after the salt had been vacuum-dried. The corresponding negative ion spectrum showed the homometallic species $[Ag_n(CN)_{n+1}]^-$ ($n = 1-3$)[2] and $[Fe(CN)_3]^-$ (also produced in ablation of $Fe^{III}[Fe^{III}(CN)_6]\cdot xH_2O$), but no $[Fe(CN)_2]^-$ (which *was* observed on ablation of $Fe^{III}[Fe^{III}(CN)_6]\cdot xH_2O$). In addition, the two new heterometallic complexes $[AgFe(CN)_4]^-$ and $[Ag_2Fe(CN)_5]^-$ were detected. CID of $[AgFe(CN)_4]^-$ (collision energy 170 eV) gave $[Fe(CN)_3]^-$ as the major product: minor species were $[Ag(CN)_2]^-$ and $[Fe(CN)_2]^-$, while CN^- became a major species at long collision times, consistent with the fact that CID of $[Fe(CN)_3]^-$ itself (collision energy 350 eV) gave CN^- (major) and $[Fe(CN)_2]^-$ (minor).

With ablation at 532 nm, the positive ion spectrum of $Ag_3[Fe(CN)_6]$ showed no evidence for cyano complexes. Only signals from K^+ (contaminant), Fe^+, and (at higher power levels) Ag^+ were observed, together with two as-yet-unidentified signals at $m/z = 277$, 339. The negative ions that were detected under these conditions were the same species found using 1064 nm irradiation.

Precursor $Ag_2[Fe(CN)_5(NO)]$. No nitrosyl complexes were detected when this salt was irradiated at either 532 or 1064 nm. Signals from a particularly wide range of homo- and heterometallic cyanometalates were observed when

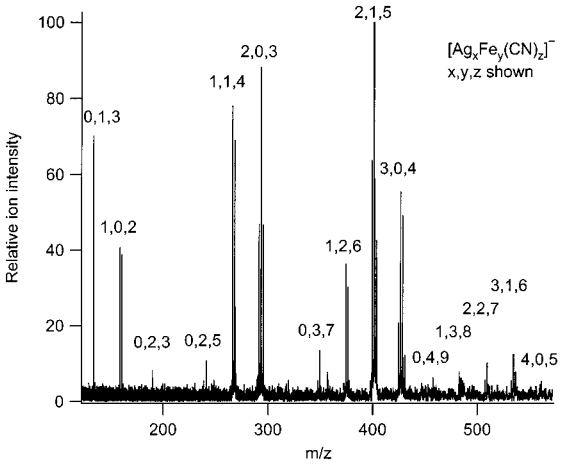

Figure 3. Negative ion mass spectrum obtained by laser ablation of $Ag_2[Fe(CN)_5(NO)]$ at 1064 nm with power density $\approx 1.8 \times 10^2$ MW cm^{-2}. Ions are formulated $Ag_xFe_y(CN)_z^-$ and identified by their indices *x*, *y*, *z*.

ablation was carried out at 1064 nm (Figure 3, Table 1). These include $[AgFe(CN)_4]^-$ and $[Ag_2Fe(CN)_5]^-$ (formed also from $Ag_3[Fe(CN)_6]$) and possibly the next member of this series, $[Ag_3Fe(CN)_6]^-$. The complexes $[Ag_nFe_2(CN)_{n+5}]^-$ can be regarded as $[Fe^{II}_2(CN)_5(Ag^ICN)_n]^-$, and this formulation adds weight to the assignment for $[Fe_2(CN)_5]^-$ itself. Similarly, the presence of $[AgFe_3(CN)_8]^-$ {$=[Fe_3(CN)_7(AgCN)]^-$} supports the occurrence of $[Fe_3(CN)_7]^-$. The corresponding positive ion spectrum is not nearly so informative. Overall, there was evidence for decomposition and/or protonation, and the only metallic species observed with certainty were Na^+, K^+, Fe^+, and Ag^+. Similarly, spectra observed using 532 nm ablation were quite uninformative. The negative ion spectra showed evidence for $[Ag_n(CN)_{n+1}]^-$ ($n = 1, 2$) and decomposition/protonation products, and only monatomic species and decomposition/protonation products could be detected in the positive ion spectra.

Precursor $Co(CN)_2$. The signal of Co^+ only is observed in the positive ion mass spectrum of laser-ablated $Co(CN)_2$. The negative ion spectrum provides good evidence for the complexes $[Co_n(CN)_{n+1}]^-$ ($n = 1$, 2, formally Co^I), $[Co(CN)_3]^-$ (Co^{II}), and $[Co_2(CN)_4]^-$ (Co^I/Co^{II}). Additional weak signals at $m/z = 280.8$ and 306.8 observed when 532 nm radiation is used with a relatively low power density (ca. 6 MW cm^{-2}) are those of $[Co_3(CN)_4]^-$ and $[Co_3(CN)_5]^-$, respectively. A CID experiment on $[Co_2(CN)_3]^-$ (collision energy 180 eV) gave mainly CN^- but also significant amounts of $[Co(CN)_2]^-$.

The species $[Co(CN)_2]^-$ and $[Co(CN)_3]^-$ (along with $[Co(CN)]^-$, which we do not observe) have been detected using TOFMS in the products of laser ablation of $K_3[Co(CN)_6]$.[19]

Precursor $Ag_3[Co(CN)_6]$. Using 1064 nm radiation for ablation, positive ions observed were the previously reported[2] $[Ag_n(CN)_{n-1}]^+$ ($n = 1-4$) and the new mixed-metal cations $[AgCo(CN)]^+$ and $[Ag_2Co(CN)_2]^+$.

The negative ion mass spectrum of $Ag_3[Co(CN)_6]$ ablated at 1064 nm shows evidence for the known[2] $[Ag_n(CN)_{n-1}]^-$ ($n = 1-3$) and all the anions observed on ablation of $Co(CN)_2$ except for $[Co_3(CN)_4]^-$ and $[Co_3(CN)_5]^-$. Also observed were Ag^- (not seen[2] in the ablation of AgCN) and the heterometallic anions $[Ag_nCo(CN)_{n+2}]^-$ ($n = 1$, 2) and $[Ag_nCo(CN)_{n+3}]^-$ ($n = 1$, 2). A CID experiment with $[AgCo(CN)_3]^-$ (collision energy 130 eV) shows that CN^-, $[Co(CN)_2]^-$, and $[Co(CN)_3]^-$ are major products and $[Ag(CN)_2]^-$ is a minor product.

The anions observed when $Ag_3[Co(CN)_6]$ was ablated using 532 nm irradiation were generally similar to those observed with ablation at 1064 nm, but the only heterometallic complex observed was $[AgCo(CN)_3]^-$. The corresponding positive ion spectra, while "clean", provided evidence for only K^+, Co^+, and Ag^+.

Precursor $Ni(CN)_2$. The positive ion mass spectrum obtained by ablation of anhydrous $Ni(CN)_2$ at 1064 nm contains signals from $[Ni_n(CN)_{n-1}]^+$ ($n = 1-3$), with the relative abundances of the cations decreasing with increasing *n*. When 532 nm radiation is used, the cation $[Ni_4(CN)_3]^+$ is observed also but with a relative abundance of less than 1%. Anions are produced according to the general formula $[Ni_n(CN)_{n+1}]^-$ ($n = 1-3$).

The occurrence of M^I only in these nickel complexes contrasts with the occurrence of a mixture of M^I and M^{II} in the gas-phase anions derived from the various cyano-species of Fe and Co, and the formation only of gaseous cyanometalates(II) from $M(CN)_2$ (M = Zn, Cd)).

Structural Chemistry of the Gas-Phase Ions. Zinc and Cadmium Complexes. In view of the common formula, $[M_n(CN)_{2n+1}]^-$, and the long series of anions that are observed for M = Zn and Cd, it seems unlikely that any major change in the coordination number or geometry of the metal centers occurs along the series. For each series, the first member, $[M(CN)_3]^-$, is expected to have trigonal planar coordination, and the stability of this geometry over alternatives has been demonstrated by density functional calculations for $[Zn(CN)_3]^-$. Accordingly, we have proposed[3] that such coordination be maintained in the larger members of the series by use of the linear cyanide bridges that are common to other extended cyanide structures involving Zn or Cd. Thus, we formulate the anions as $[(NC)_2M\{(\mu\text{-CN})M(CN)\}_{n-1}(CN)]^-$. A number of structural possibilities exist, such as the cis and trans extended sequences **1** and **2**. On

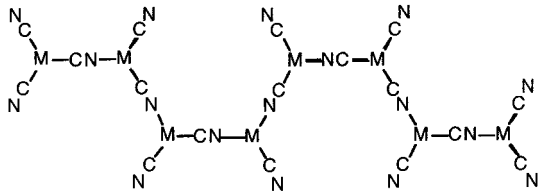

1

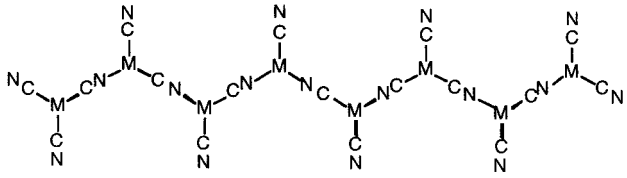

2

(19) Huang, R. B.; Wang, C.-R.; Liu, Z. Y.; Zheng, L. S.; Qi, F.; Sheng, L. S.; Yu, S. Q.; Zhang, Y. W. *Z. Phys. D: At. Mol. Clusters* **1995**, *33*, 49−52.

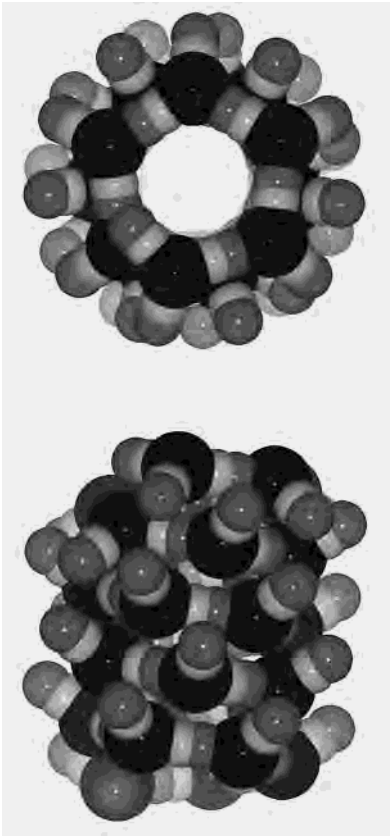

Figure 4. Axial and side views of the helical structure type calculated for ions $[M_n(CN)_{2n+1}]^-$, M = Zn, Cd: M, black; C, light gray; N, dark gray. The key feature is the location of CN from adjacent turns in the secondary axial positions of the primarily trigonal coordinate metal atoms. Analogous helices with more metals per turn are possible.[3]

the basis of (1) the enhanced abundances of middle members of the series, (2) density functional calculations of charge distributions, and (3) force field calculations, we proposed that helical structures such as that shown in Figure 4 are the most likely for ions in the series $[M_n(CN)_{2n+1}]^-$, M = Zn, Cd.[3] Details of the helical structure shown in Figure 4, including the angled conformations of the terminal CN ligands, and the juxtapositions of successive strands of the chain, are presented and justified in our previous report.[3]

The cations M^+ and M_2^+ (M = Zn, Cd) are well-established gas-phase species.

Throughout the following, the structures for $M_x(CN)_y$ are denoted **xyA**, **xyB**, **xyC**, and so forth, usually in order of decreasing stability.

Mercury Complexes. The cations Hg_x^+ (x = 1, 2) and the anion Hg^- are particularly well-known gas-phase species, but we could find no previous reports of gas phase $[Hg_x(CN)_y]$ ions. The complex $[Hg_2(CN)]^+$ is formally a mercury(I) complex and, thus, could contain a Hg-to-Hg bond. Our density functional (DF) calculations indicate that the [Hg−Hg−C−N]$^+$ structure is 20 kcal mol^{-1} more stable than [Hg−C−N−Hg]$^+$. The species $[Hg_2(CN)_2]^+$ is formally a mixed oxidation state species, Hg^I/Hg^{II}. Here, too, Hg−Hg bonding is a possibility, but DF calculations show that optimized structure **22A** without Hg−Hg is 25 kcal mol^{-1} more stable for $[Hg_2(CN)_2]^+$ than either of the two optimized Hg−Hg isomers **22B** and **22C**, or isomers **22D** (at +35 kcal mol^{-1}) and **22E** (at +58 kcal mol^{-1}).

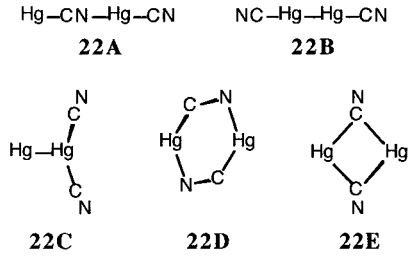

The complex $[Hg_2(CN)_3]^+$, of Hg(II), is thought to have the linear structure $[(NC)Hg(CN)Hg(CN)]^+$ in the condensed phase (see later), and DF calculations show this to be an electronically favorable structure for the gas phase.

Cyanometalates of Iron, Cobalt, and Nickel. The geometric and electronic structures of representative anionic cyanide complexes $[M(CN)_2]^-$ (M = Fe, Co, Ni), $[M(CN)_3]^-$ (M = Fe, Co), $[M_2(CN)_3]^-$ (M = Fe, Co, Ni), $[M_2(CN)_4]^-$ (M = Fe, Co), $[M_2(CN)_5]^-$ (M = Fe, Zn), $[M_3(CN)_4]^-$ (M = Co, Ni), $[Co_3(CN)_5]^-$, and $[M_3(CN)_7]^-$ (M = Fe, Zn) have been explored using density functional calculations. For some species, which are noted, there are close-lying electronic states, and for these, full characterization of the energy surfaces for both geometric and electronic structure has not been undertaken.

The calculations for $[M(CN)_2]^-$ (M = Fe, Co, Ni) showed linear or near-linear structures with C-bound terminal cyanides to be the more stable than N-bound by ca. 10 kcal mol^{-1}. On the basis of these calculations, it is assumed that any terminal cyanides in other complexes are also C-bound. The geometry-energy surface for these ions was found to be quite flat, with small deviations from linearity having insignificant effect on the binding energies.

Calculations for $[M(CN)_3]^-$ involved three structures: **13A**, trigonal planar (D_{3h}); **13B**, trigonal pyramidal (C_{3v}); and **13C**, nontrigonal planar (C_{2v}). For $[Fe(CN)_3]^-$, $[Co(CN)_3]^-$, and $[Ni(CN)_3]^-$, structure **13C** is most stable. The nonobservation of $[Ni(CN)_3]^-$ is not thought to be a consequence of an uncompetitive electronic affinity of $[Ni(CN)_3]^0$, because $[Ni(CN)_3]^0$, $[Co(CN)_3]^0$, and $[Fe(CN)_3]^0$ are calculated to have similar electron affinities, and electron attachment to $[Ni(CN)_3]^0$ is calculated to be more exergonic than to $[Ni(CN)_2]^0$, which does appear as $[Ni(CN)_2]^-$.

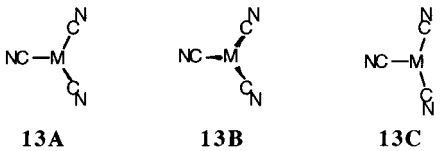

For ions of composition $[M_2(CN)_3]^-$, the structures **23A**−**E** were investigated. For Fe and Co, structure **23A** is slightly (<10 kcal mol^{-1}) more stable than **23B**, but for Ni, linear **23B** is slightly more stable than **23A**. The electronic structures of these stable species are complex, with HOMO−LUMO gaps less than 0.1 eV, and full description of the geometry-electronic-energy surface will require further cal-

culations. However, it is evident that the more bridged structures **23C**, **23D**, and **23E** are much less stable. Linear **23B** is the most stable structure for $[Cu_2CN)_3]^-$,[2] as for $[Ni_2CN)_3]^-$. In the case of $[Co_2(CN)_3]^-$, the collisionally induced dissociation to mainly CN^- and significant amounts of $[Co(CN)_2]^-$ does not differentiate structures **23A** and **23B**.

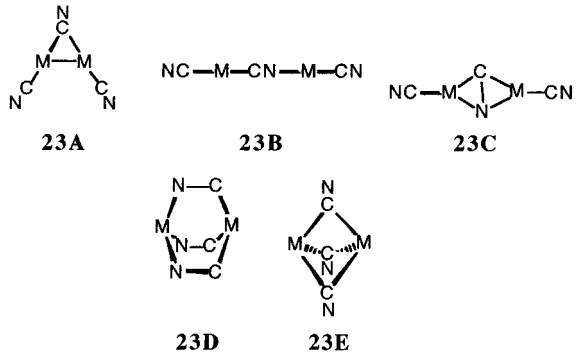

For the odd-electron composition $[M_2(CN)_4]^-$ observed for Fe and Co, the four connectivities postulated were **24A**, **24B**, **24C**, and **24D**: other cyanide bridging modes already demonstrated to be less favorable were not investigated. Some of these (**24A**, **24B**) underwent structural change during optimization without symmetry constraints. Thus, M−M bonded **24A** for Co changed stereochemistry at both M atoms, one becoming T shaped with close to linear NC−M−CN coordination, and the other M became trigonal orthogonal, as **24E**. Structure **24B** opened to **24F** for both Fe and Co, introducing additional possibilities for isomerism of C/N and isomeric stereochemistry at the M atoms, and led to **24F** as an energy minimum. For both Fe and Co, isomer **24F** is more stable than the others by ca. 20 kcal mol^{-1}. Among the other structures for iron, the isomers **24A**, **24C**, and **24E** with Fe−Fe bonding are less stable than **24D**, **24F**, and **24G** without it. For Co, the isomers **24G**, **24D**, **24E**, and **24C** all have similar energy. For the most probable structure, **24F**, the singly occupied HOMO (SHOMO) occurs at relatively high energy (−1.0 eV Fe, −1.3 eV Co), reflecting the reduced character of these species, and the SHOMO is separated from the LUMO by 0.13 eV (Fe), 0.93 eV (Co).

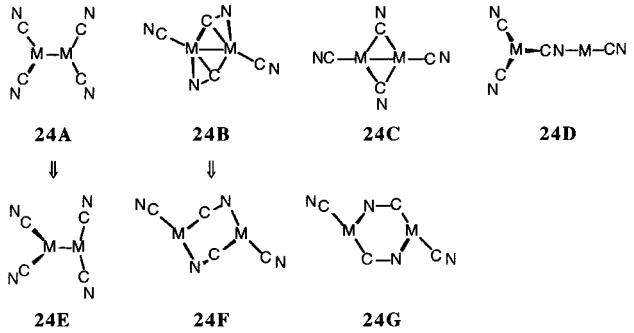

The ion $[M_2(CN)_5]^-$ was not observed for Co and Ni, even though it represents the normal M(II) oxidation state. The three connectivities explored for $Fe_2(CN)_5^-$ are **25A**, **25B**, and **25C**. Isomer **25C** is far less stable than the other two, which are very similar (∼2 kcal mol^{-1}) in energy and, as expected, have large HOMO−LUMO gaps. The optimized geometry of **25A** is strongly pyramidal at both Fe atoms, with C−Fe−C(N) angles 100−106°.

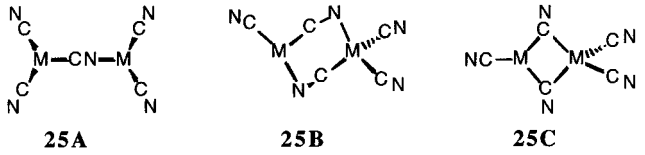

Ions $[M_3(CN)_4]^-$ were observed for M = Co, Ni, Ag. The connectivities investigated were extended **34A**, already established for Ag,[2] and double-bridged **34B** based on the favorable CN bridging found in **24F** and **25B**. For Ni, structure **34B** optimized to **34C**. Structure **34A** was the more stable for both Co (by 17 kcal mol^{-1}) and Ni (by 37 kcal mol^{-1}), and no stabilization was found for nonlinear variants of **34A**. The electronic structures of the extended linear chain of **34A** for both Co and Ni are complex, with notably high spin ground states of $S = 3$ for Co.

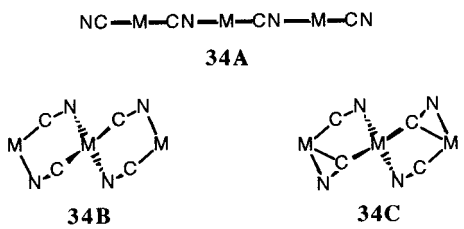

The composition $[M_3(CN)_5]^-$ was observed only for Co. Only one connectivity was explored, on the basis of the considerable stability of the **34A** structure, by addition of CN at the central Co. The preferred geometry is T-shaped at Co, as in **35A**, and again, there is a high-spin ground state, $S = {}^5/_2$. The energy surface for bending at bridging CN and at Co is very flat: for example, 70° bending at the outer Co (structure **35B**) increases the energy by only 4 kcal mol^{-1}.

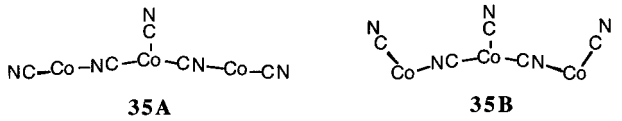

The composition $[M_3(CN)_7]^-$ is again M(II) oxidation state and was observed only for Fe and Zn. Following the principles evident from the smaller structures, connectivities with extended single bridging (**37A**) and with double bridging (**37B**) were investigated. For Fe, doubly bridged structure **37B** was the more stable, by ca. 11 kcal mol^{-1}. In contrast, for Zn, the extended structure is more stable by

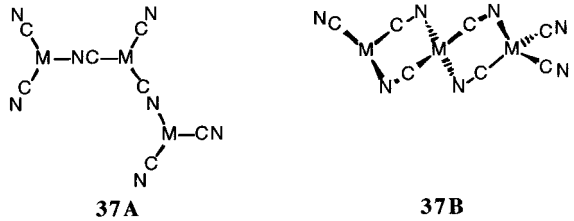

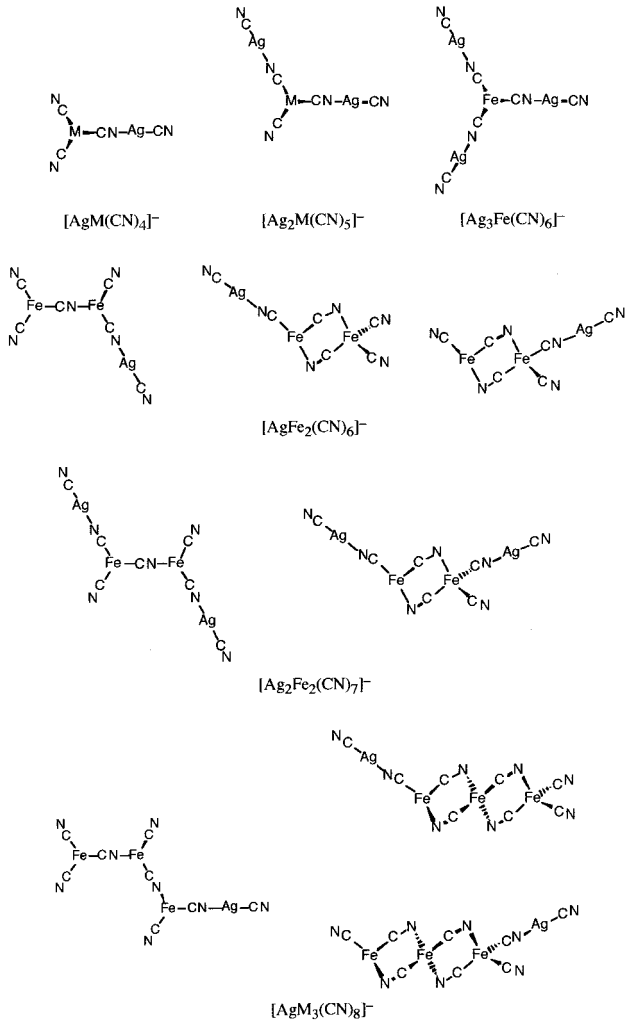

Figure 5. Structures for the heterometallic complexes, M = Co or Ni.

>25 kcal mol^{-1}, and there appears to be a barrier-free pathway from **37B** to **37A**.

Heterometallic Complexes. All of the anions listed in Table 1 as containing Fe and Ag, or Co and Ag, can be formulated as AgCN additions to the homometallic anions already discussed. Specifically, and noting the formal oxidation states, $[Ag_nFe(CN)_{n+3}]^-$ is $[Fe^{II}(CN)_3]^-\cdot nAg^{I}CN$, $[Ag_nFe_2(CN)_{n+5}]^-$ is $[Fe^{II}_2(CN)_5]^-\cdot nAg^{I}CN$, $[AgFe_3(CN)_8]^-$ is $[Fe^{II}_3(CN)_7]^-\cdot Ag^{I}CN$, $[Ag_nCo(CN)_{n+2}]^-$ is $[Co^{I}(CN)_2]^-\cdot nAg^{I}CN$, and $[Ag_nCo(CN)_{n+3}]^-$ is $[Co^{II}(CN)_3]^-\cdot nAg^{I}CN$. By analogy with the proposed[2] linear structures of $[Ag_n(CN)_{n-1}]^+$ and $[Ag_n(CN)_{n+1}]^-$, such formulations suggest structures with AgCN attached at terminal CN ligands, to generate linear terminal moieties NCAgNCM− or NCAgCNM−. Using the structural findings for the homometallic anionic species, structures for the heterometallic anions are then readily proposed, as in Figure 5 (M = Fe or Co) for $[AgM(CN)_4]^-$, $[Ag_2M(CN)_5]^-$, $[Ag_3Fe(CN)_6]^-$, $[AgFe_2(CN)_6]^-$, $[Ag_2Fe_2(CN)_7]^-$, and $[AgM_3(CN)_8]^-$.

The collisionally induced dissociation (CID) of $[AgFe(CN)_4]^-$ yielded $[Fe(CN)_3]^-$ (major) and $[Fe(CN)_2]^-$ and $[Ag(CN)_2]^-$ (minors), plus CN^-, entirely consistent with the structure proposed. The heterometal species $[AgCo(CN)_3]^-$ and $[Ag_2Co(CN)_4]^-$ are formally AgCN adducts of $[Co(CN)_2]^-$. However, the CID of $[AgCo(CN)_3]^-$ includes the fragments $[Co(CN)_3]^-$, $[Co(CN)_2]^-$, and CN^- (all major) and $[Ag(CN)_2]^-$ (minor). Here, the formation of $[Ag(CN)_2]^-$ is consistent with a straight-chain structure NC−Ag−(CN)−Co−CN, but this structure does not account for the formation of $[Co(CN)_3]^-$. Therefore, it seems that $[AgCo(CN)_3]^-$ can exist with structures other than the expected extended chain, and DF calculations were applied to this question. The three structures considered for $[AgCo(CN)_3]^-$ are **AgCoA**, **AgCoB**, **AgCoC**. **AgCoB** is the only single structure consistent with the CID data, but the DF calculations indicate that it is 28 kcal mol^{-1} less stable than the extended chain, and uncertainty remains about the structure(s) of $[AgCo(CN)_3]^-$.

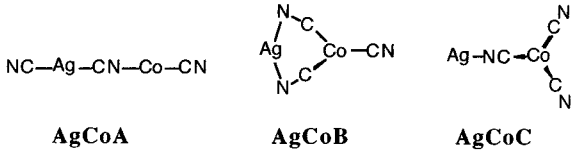

AgCoA 0 | **AgCoB** +28 kcal mol^{-1} | **AgCoC** +39 kcal mol^{-1}

Discussion

We have shown that anionic binary and ternary metal cyanide complexes can be generated in the gas phase for metals in groups 8−12 of the periodic table. Extended series $[M_n(CN)_{2n+1}]^-$ occur for Zn and Cd, containing up to 27 (Zn) or 30 (Cd) metal atoms, and these have been interpreted in terms of the formation of helices in the gas phase. For Cu and Ag, extended linear rods are probable. In both series, the formal oxidation states of the complexes are normal. For Hg, the compositions and calculations provide no indication that Hg−Hg bonded complexes are stabilized in the gas phase, except in the mercurous complex $[Hg-Hg-CN]^+$. For the transition metals, the sizes of $[M_x(CN)_y]^-$ complexes in the gas phase are restricted in our experiments, the largest being $[Fe_3(CN)_7]^-$, although there is a trace of $[Fe_4(CN)_9]^-$. Experiments allowing the formation of mixed Fe + Ag species, and of Co + Ag species, generate complexes that can be interpreted as having AgCN moieties added to terminal CN of the homometallic complexes, generating M−CN−Ag−CN sections.

Density functional calculations provide general insight into the probable structures of the transition complexes in the gas phase. The compositions of the complexes result in undercoordination of the metals relative to the norm for condensed phases. Cyanide bridging is prevalent, in preference to metal−metal bonding (the exception is Fe-**23A**). The two favored bridge geometries are linear M−CN−M (**B1**) for single bridges and **B2** for double bridges. We note that η^1-CN bridging (**B3**) is not supported by the calculations. In general, the double cyanide bridging increases the otherwise low coordination numbers of the metal atoms, but this does not provide marked energy stabilization, and this is probably because the geometry of the double bridge **B2** diminishes the quality of overlap and interaction between the CN orbitals (particularly at N) and metal orbitals. Most generally, it appears that the structures proposed involve a

compromise between increased metal coordination with poorer (double, **B2**) cyanide bridging and reduced metal coordination with better (single, **B1**) cyanide bridging. For $[M_2(CN)_4]^-$, the double bridging allowing three-coordination of both metals is more stable, and double bridging occurs in the better of the two structures for $[Fe_3(CN)_7]^-$, while single bridging is calculated to be more favorable for $[M_3(CN)_4]^-$ (Co, Ni), and there is no significant difference between the two structure types for $[M_2(CN)_5]^-$ (Co, Ni).

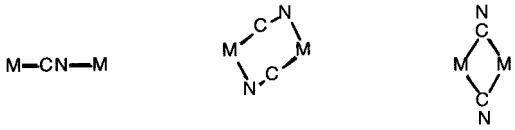

B1 **B2** **B3**

Another general result is that three-coordinate transition metals adopt stereochemistries other than trigonal planar, namely trigonal pyramidal and T-shaped: C/N isomerism in **B1** is not a significant energy discriminator.

The electronic structure and electronic population of the gaseous transition metal cyanide complexes are significant in several ways. Formal oxidation states in the gaseous complexes are sometimes subnormal (relative to the condensed phase), as analyzed in more detail later. In a number of cases, particularly linear complexes with **B1** bridges, it appears that the electronic structure involves close-lying or degenerate orbitals at the Fermi level, and there are potentially complex electronic states which have not been probed in detail here. Further, we note that a number of the species are predicted to be high spin, particularly the extended linear chain structures of Co and Ni.

In the following section, we compare the structural and redox chemistry of gaseous and condensed phase systems, before considering possibilities for the crystallization of new compounds and structures inspired by the gas-phase results.

Comparison with Condensed Phases

In condensed phases, as in the gas phase, the chemistry of zinc and cadmium with CN^- as a ligand involves the metal in the +II oxidation state exclusively. Although the species $[M(CN)]^+(g)$ (M = Zn, Cd) are new, stability constant data are available for $[M(CN)]^+(aq)$.[7f] The anions $[M(CN)_x]^{(x-2)-}$ (M = Zn or Cd; $x = 3, 4$) are known in solution.[7f] However, for M = Zn, only salts of $[Zn(CN)_4]^{2-}$ have been characterized structurally in the solid state.[7f] For M = Cd, solid-state structural data have been reported[7f,20] for the discrete anions $[Cd(CN)_4]^{2-}$ and cyanide-bridged $[(NC)_3Cd-CN-Cd(CN)_3]^-$. A salt of formula $(Ph_4Sb)[Cd(CN)_3]$ contains an infinite anionic chain with tetrahedral coordination of the metal ion.[21] In addition, polymeric anions of formulas $[Cd_3(CN)_7]^-$ and $[Cd_4(CN)_9]^-$ are known as metal complex hosts in a variety of clathrate compounds.[22] Solid $Zn(CN)_2$ and $Cd(CN)_2$ have the anti-Cu_2O structure, with tetrahedrally coordinated metal ions connected via bridging cyanides M−CN−M.[23a]

Several of the Hg/CN stoichiometries that we observe for gas-phase species have been established in condensed phases. Thus, the cation $[Hg_2(CN)_3]^+$, considered to be linear, is produced from $Hg(CN)_2$ in HF(l),[24] while $Hg/CN^- = 1/1$ is known only as nonmolecular $[Hg(CN)^+]_\infty$ that occurs in $Hg(CN)(NO_3)$[25] and is likely to occur in the salts $Hg(CN)(BF_4)$ and $Hg(CN)(AsF_6)$.[24] Similar strong (near-)linear bonding is found in the structure of $Hg(CN)_2(s)$ itself.[23b] The anion $[Hg(CN)_3]^-$ has been shown to occur in various solvents.[7g,26] This ion is found in planar form, with weak interionic Hg··N bonding, in the structure of $CsHg(CN)_3$.[27] On the other hand, the cation $[Hg_2(CN)]^+(g)$ and the anion $[Hg(CN)_2]^-(g)$ have no counterparts in condensed phases, because CN^- causes disproportionation of Hg(I). Similarly, the species $[Hg_2(CN)_2]^+(g)$ is unknown in condensed phases. However, instances of formally Hg(I)/Hg(II) complexes of Hg are known, for example, the cation $[Hg_3(dppm)_3]^{4+}$ (dppm = 1,2-bis(diphenylphosphino)methane),[28] and involve Hg-to-Hg bonding.

The production of gaseous complexes containing, formally, Fe(I) and/or Fe(II) from Fe(III) precursors ($Fe^{III}[Fe^{III}(CN)_6]\cdot xH_2O$ and $Ag_3[Fe(CN)_6]$) is noteworthy. Homoleptic Fe(I)/CN^- complexes are not well established, in contrast to their Fe(II) and Fe(III) analogues.[7h,29] We note the occurrence of reduced Fe−CN moieties at the FeNi and Fe_2 active sites of hydrogenase enzymes.[30]

None of the Co(I) or Co(II) complexes described in the present work or in ref 19 have analogues in condensed phases. However, there is evidence for the occurrence of Co(I)/CN^- complex $[Co(CN)_5]^{4-}$ as an intermediate in a variety of experiments,[7i,31] and a salt formulated $K_3Co^I(CN)_4$ has been synthesized but not yet fully characterized.[32] For

(20) Kitazawa, T.; Takeda, M. *J. Chem. Soc., Chem. Commun.* **1993**, 309−310.
(21) Kitazawa, T.; Akiyama, M.; Takashi, M.; Takeda, M. *J. Chem. Soc., Chem. Commun.* **1993**, 1112−1113.
(22) Kitazawa, K.; Nishikiori, S.; Kuroda, R.; Iwamoto, T. *Chem. Lett.* **1988**, 459−462. Iwamoto, T. In *Inclusion Compounds*; Atwood, J. L., Davies, J. E. D., MacNicol, D. D., Eds.; Oxford University Press: Oxford, 1991; Vol. 5; pp 202. Kitazawa, K.; Nishikiori, S.; Iwamoto, T. *J. Chem. Soc., Dalton Trans.* **1994**, 3695−3710.
(23) Wells, A. F. *Structural Inorganic Chemistry*, 5th ed; Clarendon: Oxford, 1984. (a) Page 941 and references therein. (b) Page 943 and references therein.
(24) Gillespie, R. J.; Hulme, R.; Humphreys, D. A. *J. Chem. Soc.A* **1971**, 3574−3578.
(25) Mahon, C.; Britton, D. *Inorg. Chem.* **1971**, *10*, 2331−2333.
(26) Brodersen, K.; Hummel, H. U. In *Comprehensive Coordination Chemistry*; Wilkinson, G., Gillard, R. D., McCleverty, J. A., Eds.; Pergamon: Oxford, 1987; Vol. 5; pp 1062 ff.
(27) Thiele, G.; Bauer, R.; Messer, D. *Naturwissenschaften* **1974**, *61*, 215−216.
(28) Hammerle, B.; Muller, E. P.; Wilkinson, D. L.; Muller, G.; Peringer, P. *J. Chem. Soc., Chem. Commun.* **1989**, 1527−1528. Knoepfler-Muhlecker, A.; Scheffter, B.; Kopacka, H.; Wurst, K.; Peringer, P. *J. Chem. Soc., Dalton Trans.* **1999**, 2525. Knoepfler-Muhlecker, A.; Ellmerer-Muller, E.; Konrat, R.; Ongania, K.-H.; Wurst, K.; Peringer, P. *J. Chem. Soc., Dalton Trans.* **1997**, 1607.
(29) Hawker, P. N.; Twigg, M. V. In *Comprehensive Coordination Chemistry*; Wilkinson, G., Gillard, R. D., McCleverty, J. A., Eds.; Pergamon: Oxford, 1987; Vol. 4, pp 1201 ff and references therein.
(30) Peters, J. W. *Curr. Opin. Struct Biol.* **1999**, *9*, 670−676. Siegbahn, P. E. M.; Blomberg, M. R. A.; Wirstam, M.; Crabtree, R. H. *J. Biol. Inorg. Chem.* **2001**, *6*, 460−466. Fan, H.-J.; Hall, M. B. *J. Biol. Inorg. Chem.* **2001**, *6*, 467−473.

Co(II), $[Co(CN)_4]^{2-}$ [33,34] and both monomeric[35] and dimeric[36] complexes with Co(II)/CN^- = 1/5 have been characterized structurally, and $[Co(CN)_x]^{(x-2)-}$ ($x = 1-5$) occur in polar aprotic solvents.[34] Again, it is significant that ablation of a cyano complex of Co(III), $Ag_3[Co(CN)_6]$, yields only complexes with lower oxidation states of Co, Co(I) and Co(II).

The new complexes $[Ni_n(CN)_{n-1}]^+$ ($n > 1$) and $[Ni_n(CN)_{n+1}]^-$ are produced from a Ni(II) precursor, $Ni(CN)_2$, with no evidence for coproduction of Ni(II) species. A few examples of Ni(I)/CN^- complexes are extant. Salts in which Ni(I)/CN^- = 1/3 contain Ni−Ni bonded $[(NC)_3Ni\text{-}Ni(CN)_3]^{4-}$.[37] A compound formulated as $K_3[Ni^I(CN)_4]$ is still incompletely characterized.[7i,38]

In summary, with the exception of $M(CN)_2$ (M = Zn or Cd), ablation of the cyano species that we have used as precursors yields some or all species with a lower metal oxidation state than in the precursor. With or without a change in oxidation state, most of the discrete gas-phase complexes that are observed are unknown in condensed phases. When gaseous and condensed phase cyano complexes of Co(I) and Ni(I) are compared, the CN^-/M ratio is smaller in the gas phase.

The findings reported here provide inspiration for the further development of cyano−metalate complexes in the condensed phases, by careful control of the associated cations and the crystallization conditions. The helical structures and the rod structures are not yet established in crystals, and neither is the bridge **B2**. There are indications that rod or extended structures such as **34A**, **35A** with the transition metals will possess significant electronic structures with the possibilities of electron conduction and/or high spin molecular magnetism. An unusually high molecular spin state is already established in cyanide bridged $[Mn\{Mn(MeOH)_3\}_8(\mu\text{-}CN)_{30}\{Mo(CN)_3\}_6]$.[4]

Acknowledgment. This research was supported by the Australian Research Council and the Natural Sciences and Engineering Research Council of Canada. P.A.W.D., Honorary Visiting Professor at UNSW, is grateful to the University of Western Ontario for sabbatical leaves and a leave of absence, during which this work was completed. H.H.H. acknowledges an Australian Postgraduate Award.

Supporting Information Available: Table of anionic carbon−nitride anions observed, with details of their collision-induced dissociation (CID) products. This material is available free of charge via the Internet at http://pubs.acs.org.

IC011227D

(31) Buckingham, A. D.; Clark, C. R. In *Comprehensive Coordination Chemistry*; Wilkinson, G., Gillard, R. D., McCleverty, J. A., Eds.; Pergamon: Oxford, 1987; Vol. 4, pp 6446 ff and references therein.
(32) Watt, G. D.; Thompson, R. J. *J. Inorg. Nucl. Chem.* **1959**, *9*, 311−314.
(33) Carter, S. J.; Foxman, B. M.; Stuhl, L. S. *J. Am. Chem. Soc.* **1984**, *106*, 4265−4266.
(34) Carter, S. J.; Foxman, B. M.; Stuhl, L. S. *Inorg. Chem.* **1986**, *25*, 2888−2894.
(35) Brown, L. D.; Raymond, K. N. *Inorg. Chem.* **1975**, *14*, 2590−2594.
(36) Simon, G. L.; Adamson, A. W.; Dahl, L. F. *J. Am. Chem. Soc.* **1972**, *94*, 7654−7663. Brown, L. D.; Raymond, K. N.; Goldberg, S. Z. *J. Am. Chem. Soc.* **1972**, *94*, 7664−7674.
(37) Jarchow, O.; Schuttz, H.; Nast, R. *Angew. Chem., Int. Ed. Engl.* **1970**, *9*, 71. Jarchow, O. *Z. Anorg. Allg. Chem.* **1971**, *383*, 40−48.
(38) Nast, R.; Trakkay, T. *Z. Naturforsch., B: Chem. Sci.* **1954**, *9*, 78−79. Sacconi, L.; Mani, F.; Bencini, A. In *Comprehensive Coordination Chemistry*; Wilkinson, G., Gillard, R. D., McCleverty, J. A., Eds.; Pergamon: Oxford, 1987; Vol. 5; p 37.